Chemical Science

ROYAL SOCIETY OF CHEMISTRY

REVIEW

View Article Online
View Journal | View Issue

Cite this: *Chem. Sci.*, 2024, **15**, 12189

Strategies to boost the electrochemical performance of bismuth anodes for potassium-ion batteries

Xunzhu Zhou,‡[abc] Xiaomin Chen,‡[a] Wenxi Kuang,[c] Xiaosa Zhang,[a] Xingqiao Wu,[ac] Xiang Chen,[d] Chaofeng Zhang,*[b] Lin Li*[ac] and Shu-Lei Chou*[ac]

Received 17th May 2024
Accepted 28th June 2024

DOI: 10.1039/d4sc03226h

rsc.li/chemical-science

Potassium-ion batteries (PIBs) are considered potential candidates for large-scale energy storage systems due to the abundant resources of potassium. Among various reported anode materials, bismuth anodes with the advantages of high theoretical specific capacity, low cost, and nontoxicity have attracted widespread attention. However, bismuth anodes experience significant volume changes during the charge/discharge process, leading to unsatisfactory cycling stability and rate performance. In this review, we focus on summarizing the research progress of bismuth anodes in PIBs. We discuss in detail the modification strategies for bismuth anodes in PIBs, including electrolyte optimization, morphology design, and hybridization with carbon materials. In addition, we attempt to propose possible future directions for the development of bismuth anodes in PIBs, aiming to expedite their practical application. It is believed that this review can assist researchers in more efficiently designing high-performance bismuth anode materials for PIBs.

1. Introduction

The quest for sustainable energy storage solutions has been a priority in scientific research due to the escalating demand for renewable energy sources (such as wind and solar energy) and the need to reduce carbon emissions. Lithium-ion batteries (LIBs) have been at the forefront of this revolution, and are widely used in portable electronic devices and electric vehicles.[1–3] However, the limited availability and uneven distribution of lithium resources hinder the application of LIBs in

[a]*Institute for Carbon Neutralization Technology, College of Chemistry and Materials Engineering, Wenzhou University, Wenzhou, Zhejiang 325035, China. E-mail: linli@wzu.edu.cn; chou@wzu.edu.cn*

[b]*Institute School of Materials Science and Engineering, Institutes of Physical Science and Information Technology, Leibniz Joint Research Center of Materials Sciences, Key Laboratory of Structure and Functional Regulation of Hybrid Material (Ministry of Education), Anhui University, Hefei, Anhui 230601, China. E-mail: cfz@ahu.edu.cn*

[c]*Wenzhou Key Laboratory of Sodium-Ion Batteries, Wenzhou University Technology Innovation Institute for Carbon Neutralization, Wenzhou, Zhejiang 325035, China*

[d]*College of Textile Science and Engineering (International Institute of Silk), Zhejiang Sci-Tech University, Hangzhou 310018, PR China*

‡ Theses authors contributed equally to this work.

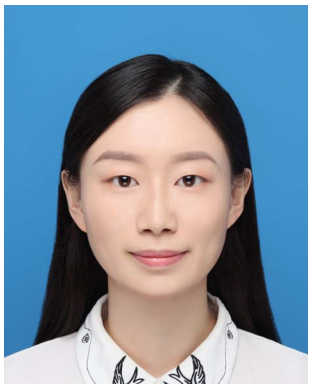

Xunzhu Zhou

Xunzhu Zhou received her PhD degree (2022) from the College of Chemistry, Nankai University. After that, she started working as a postdoctoral researcher at the Institutes of Physical Science and Information Technology, Anhui University. Her research mainly focuses on the mechanism and behavior of electrode–electrolyte interface reactions.

Xiaomin Chen

Xiaomin Chen is currently an M.E. candidate at the College of Chemical and Materials Engineering, Wenzhou University. Her research interest is focused on the advanced electrolyte design for sodium-ion batteries.

large-scale storage systems. Therefore, developing battery systems based on elements with high crustal abundance is of great significance, such as sodium (Na), potassium (K), magnesium (Mg), calcium (Ca), zinc (Zn), and aluminum (Al).[4–9]

Among these, potassium ion batteries (PIBs) have attracted widespread attention due to the low standard redox potential of potassium metal (−2.93 V *vs.* standard hydrogen electrode).[10] In addition, potassium is much more abundant in the Earth's crust than lithium, which could significantly reduce the overall cost of battery production. Potassium does not form alloys with aluminum, allowing aluminum to replace copper as the anode current collector.[11] More importantly, the weaker Lewis acidity and larger ionic radius of K^+ compared to Li^+ and Na^+ result in weaker interactions with organic solvents, which is beneficial for rapid energy storage and conversion.[12,13] Therefore, PIBs are considered a highly potential energy storage technology for large-scale energy storage systems.

PIBs operate on a similar principle to LIBs, where ions move between the anode and cathode during the charge/discharge process (Fig. 1). The development of PIBs can be traced back to 2004 when Eftekhari's group constructed a potassium secondary battery by employing a Prussian blue-based cathode and potassium metal.[14] Over the past few decades, significant progress has been made in the development of PIBs, but numerous challenges still hinder their practical application. One of the main challenges was the large ionic radius of K^+, which leads to slow electrochemical reaction kinetics and significant volume changes.[15–17] These generate an unsatisfactory rate performance and cycling stability. Therefore, many researchers have been dedicated to developing electrode materials with rapid ion transport pathways and excellent structural stability. Various cathode materials (including Prussian blue, polyanion, metal oxide, and organic materials) have been applied for PIBs, showing satisfactory electrochemical performance.[18–21] On the anode side, graphite anodes used in commercial lithium-ion batteries have been proven to serve as anodes for PIBs.[22] However, the theoretical capacity of graphite

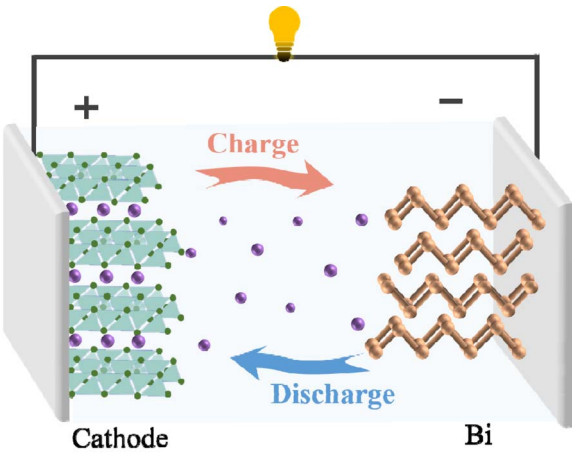

Fig. 1 Schematical illustration of the working mechanism of PIBs.

is 279 mA h g^{-1}, which hardly meets the demands of practical applications. The potassium storage performance of the commonly used anodes in LIBs and SIBs was investigated, such as carbon materials, organic materials, Sb, Sn, Bi, P, *etc.*[23–28] Among these, Bi anodes with the merits of high theoretical capacity, low cost, and nontoxicity have attracted widespread attention.[29] In addition, Bi anodes deliver a suitable potential (~0.5 V *vs.* K^+/K), enabling the safety of PIBs.[30] Nevertheless, Bi anodes undergo a huge volume change to induce pulverization during the charge/discharge process, which leads to poor cycling stability.[31] Until now, various effective strategies have been applied to overcome this issue to realize superior electrochemical performance. Therefore, comprehensively summarizing the recent advancements of the bismuth anode is highly significant for promoting its practical applications in PIBs.

In this review, we will focus mainly on the recent advances in Bi anodes for PIBs. We summarize the advanced strategies to boost the potassium storage performance of Bi anodes (such as

Chaofeng Zhang

Chaofeng Zhang is currently a professor at the Institutes of Physical Science and Information Technology, Anhui University, Hefei, China. He received his BSc and M.Sc. from Lanzhou University and Fudan University, respectively. Then, he obtained his PhD degree in 2013 from the University of Wollongong, Australia. Additionally, he was a post-doc at the National Institute of Advanced Industrial Science and Technology (AIST), Japan. His research focuses on electrochemistry for batteries, especially organic battery materials and electrolytes of aqueous zinc-ion batteries.

Lin Li

Lin Li is an Oujiang Distinguished Professor and an Associate Dean of the Institute for Carbon Neutralization Technology, College of Chemistry and Materials Engineering, Wenzhou University. He received his B.S. degree in materials science and engineering from Nanchang University (2016). He obtained his PhD from Nankai University in 2021. His research focuses on advanced electrode materials and electrolytes for rechargeable batteries.

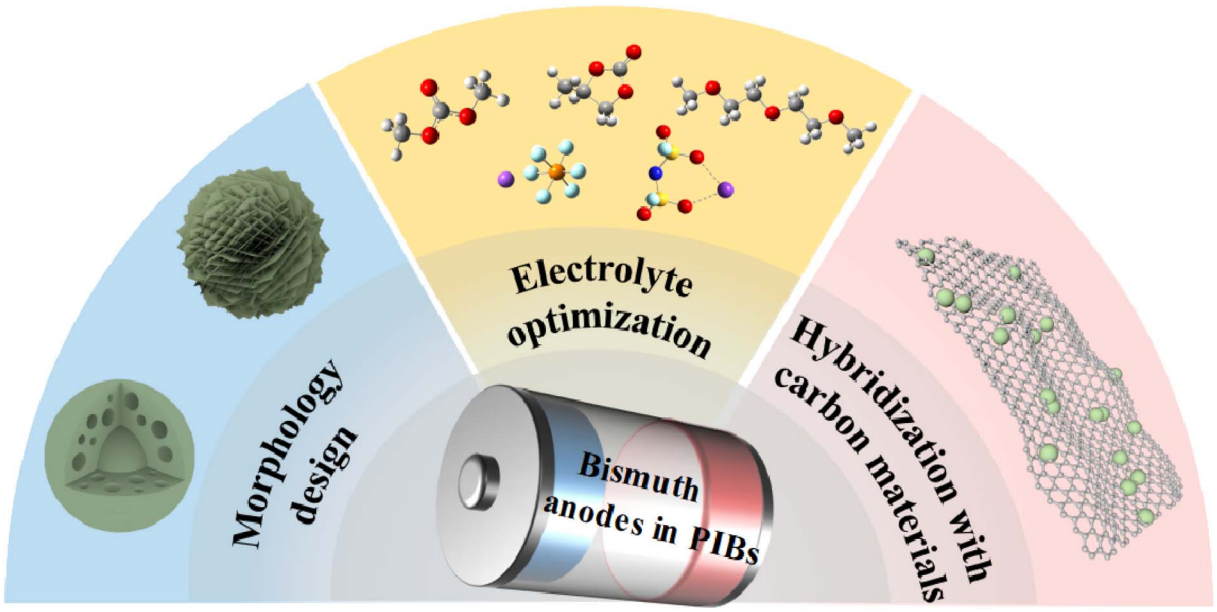

Fig. 2 Strategies to boost the potassium storage performance of Bi anodes.

electrolyte optimization, morphology design, and hybridization with carbon materials). In addition, we attempt to provide insights into the research and application of Bi anode materials for high-performance PIBs.

2. Strategies to boost electrochemical performance

The main challenge faced by bismuth anodes is the substantial volume expansion during the charge/discharge process, which

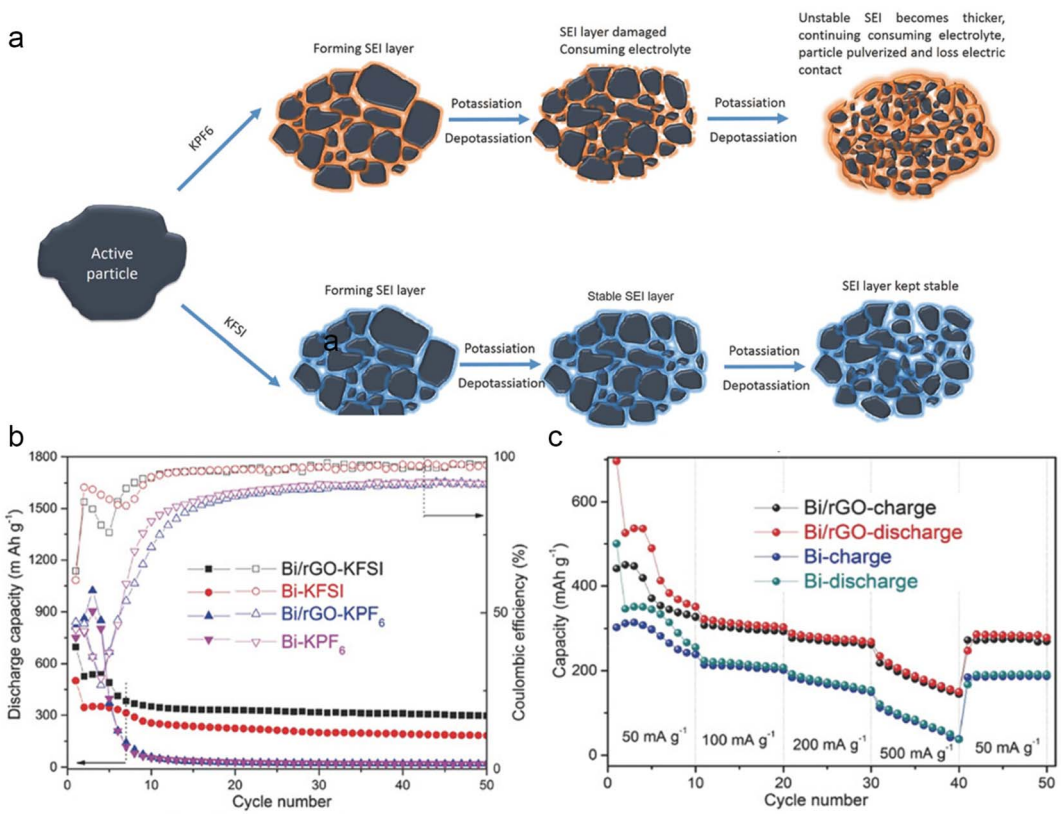

Fig. 3 (a) Schematic illustration of the SEI layer on the surface of the Bi/rGO electrode in different electrolytes. (b) Cycling stability of Bi and Bi/rGO electrodes in KPF_6 and KFSI-based electrolytes. (c) Rate performance of Bi and Bi/rGO in a KFSI-based electrolyte. Reproduced with permission.[32] Copyright 2018, Wiley-VCH.

leads to material pulverization and consequently deteriorates the electrochemical performance. Currently, researchers have proposed various strategies to overcome this problem, which can be broadly categorized into three categories: electrolyte optimization, morphology design, and hybridization with carbon materials (Fig. 2). These strategies can effectively enhance the initial Coulombic efficiency, reversible capacity, cycling stability, and rate performance of bismuth anodes. We subsequently discussed in detail the recent achievements of these strategies to boost the potassium storage performance of bismuth anodes. Since some studies applied two or more strategies, we primarily describe the impact of a single strategy on the electrochemical performance when categorizing them.

2.1 Electrolyte optimization

The electrolyte plays a crucial role in the formation and stability of the solid electrolyte interphase (SEI) layer, which directly impacts the electrochemical performance of electrode materials. The effect of potassium salts on the potassium storage performance of Bi metal was investigated by Guo's group.[32] They found that the potassium storage performance was significantly improved by employing potassium bis(fluorosulfonyl)imide (KFSI) to replace potassium hexafluorophosphate (KPF_6) in the carbonate electrolyte. Compared with KPF_6, KFSI is more advantageous in terms of constructing a uniform and stable SEI layer with superior mechanical and electrical properties (Fig. 3a). This characteristic helps to prevent the successive decomposition of electrolytes and maintains the integrity of the electrode. As shown in Fig. 3b and c, the Bi electrode has shown better cycling stability and rate performance in KFSI-based electrolytes. Furthermore, the effectiveness of this strategy has been confirmed in Sn and Sb metals, showcasing its universality in different anode materials. It's worth noting that the high cost of KFSI salt makes it challenging for practical application. Therefore, the development of low-cost and high-performance potassium salts is very significant. In addition, Sun and co-workers discovered that the concentration of salts significantly impacts the electrochemical performance of Bi metal.[33] They found that the reduction resistance of electrolytes was

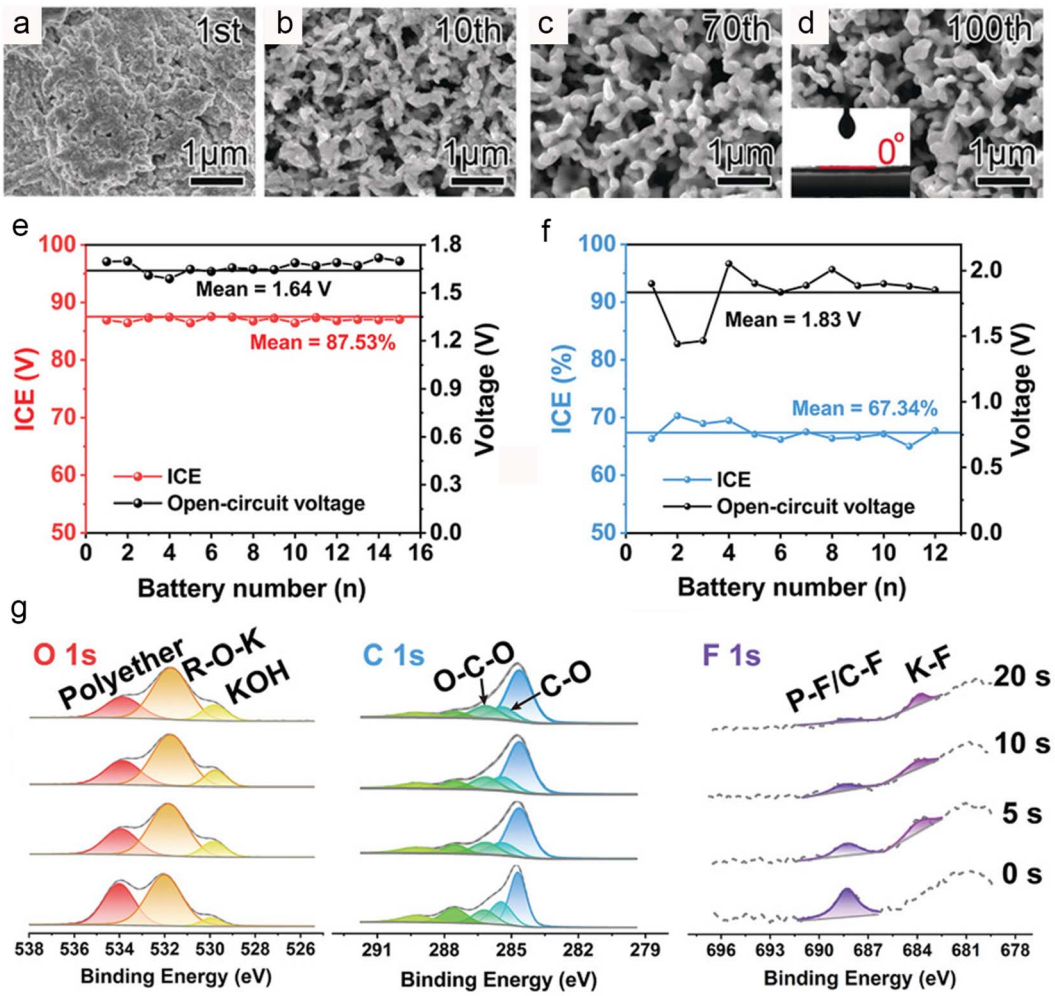

Fig. 4 (a–d) SEM images of cycled Bi electrodes. Inset: contact angle of a DME-based electrolyte on the Bi electrode. Reproduced with permission.[34] Copyright 2018, Wiley-VCH. ICE and OCV of the 2D-Bi in an (e) ether-based electrolyte and (f) ester-based electrolyte. (g) XPS of the 2D-Bi electrodes after cycling in the ether-based electrolyte. Reproduced with permission.[35] Copyright 2021, Wiley-VCH.

improved with salt concentration. The concentrated electrolyte with elevated reduction resistance can effectively passivate the surface of bismuth metal to avoid the continuous decomposition of the electrolyte. Therefore, the bismuth anode delivers a high capacity retention of 85% even after 600 cycles. However, the high viscosity and cost of the concentrated electrolyte pose serious constraints on its practical applications.

Solvent, as an essential component of electrolytes, also has a significant impact on the electrochemical performance of electrode materials. For example, Li's group demonstrated that the use of ether-based electrolytes can significantly enhance the electrochemical performance of bismuth metal.[34] Scanning electron microscopy images revealed that ether-based electrolytes can induce the *in situ* formation of a porous network in bismuth metal, thereby achieving rapid electrochemical reaction kinetics and accommodating volume changes during charge/discharge processes (Fig. 4a–d). Density functional theory calculations reveal that the formation of the porous network is closely related to the strong chemical adsorption of DME on Bi. Benefiting from the unique porous network, the anode exhibits excellent rate performance and cycling stability in ether-based electrolytes. Additionally, the Bi//$K_{0.72}Fe[Fe(CN)_6]$ full cell delivers high energy density (108.1 W h kg^{-1}) and good cycling stability (a capacity retention of 85% after 350 cycles), demonstrating the practical application potential of the bismuth anode in PIBs. However, the mechanism of the *in situ* porous evolution of microsized Bi during the charge/discharge process is not clear. Recently, Zheng's group proposed that the porous evolution of Bi was closely related to the interfacial charge distribution on the Bi surface, a uniform interfacial charge distribution induces a unique 3D porous network.[36]

In addition, Zhang *et al.* also found that ether-based electrolytes can effectively enhance the potassium storage performance of bismuth anodes.[37] However, they believe that the improvement in electrochemical performance is mainly due to the formation of an elastic and adhesive oligomer-containing SEI in ether-based electrolytes. Subsequently, Yu's group disclosed the impact of solvents on the initial Coulombic efficiency of bismuth metal anodes.[35] As shown in Fig. 4e and f, the bismuth anodes in ether-based electrolytes demonstrate significantly higher initial Coulombic efficiency compared to ester-based electrolytes. XPS results suggest that ether-based electrolytes favor the formation of a thin and dense SEI layer containing polyether, fluorinated organic compounds and KF (Fig. 4g), thereby preventing the continuous decomposition of the electrolyte and achieving high initial Coulombic efficiency. Recently, Zheng and co-workers prepared a nanostructured Bi@N-doped carbon (Bi@NC) bulk anode and systematically studied its interfacial ion transport behavior.[38] Impedance spectroscopy studies indicated that the transport of K^+ through the SEI layer plays a pivotal role in interfacial K^+ transfer. Moreover, they discovered that the interaction between the Bi@NC anode and ether-based electrolytes can generate a unique SEI layer containing the Bi^{3+}–solvent complex, thereby achieving a low interfacial K^+ transfer activation energy of 25.9 kJ mol^{-1}. Therefore, the bismuth anode demonstrated excellent rate performance (a reversible capacity of 206 mA h g^{-1} at 120 C) and cycling stability (a capacity retention of 81.8% even after 1400 cycles). For the practical application, the compatibility of ether electrolytes with high-voltage cathodes should be further investigated in potassium-ion full batteries.

2.2 Morphology design

The enhancement of the electrochemical performance of electrode materials through morphology design was extensively applied in the field of energy storage technologies. In 2019, Ma and co-workers designed mesoporous carbon-coated Bi (Bi@C) nanorods for PIBs.[39] The unique core–shell structure enables a significantly improved rate performance and cycling stability. Subsequently, Bi nanorods encapsulated in a hollow N-doped carbon nanotube (Bi@N-CT) were prepared by Jian's group.[40] The unique structure of bismuth nanorods provides shorter K^+ transport paths compared to micronsized Bi. Meanwhile, the gaps between bismuth nanorods and carbon nanotubes can alleviate volume changes during the charge/discharge process. As a result, the Bi@N-CT electrode exhibits superior cycling stability (capacity retention of 88% after 1000 cycles) and rate performance (297 mA h g^{-1} at 20 C). Zhang's group constructed a nanostructure Bi-based composite containing Bi nanorod networks confined in a robust N, S co-doped carbon matrix (Bi@NS-C).[41] The unique Bi nanorod networks effectively improved the electrochemical kinetics and maintained the integrity of the electrode, and then realized an excellent potassium storage performance. In addition, the PB//Bi@NS-C full cells exhibit a high energy density of 295 W h kg^{-1} and outstanding cycling stability, suggesting that Bi@NS-C is a promising candidate for PIBs.

Carbon-coated double-shell structured bismuth hollow boxes (C@DSBC) were synthesized by Qiao's group.[42] Compared to microsized bismuth anodes, C@DSBC exhibited higher reversible capacity, excellent cycling stability, and rate performance. The origin of the improved reversible capacity of C@DSBC was investigated by *in situ* XRD and *ex situ* XANES. The results indicated that at low current densities, the unique nanostructure of C@DSBC accommodates larger volume expansion enabling more complete alloying reactions, leading to a higher reversible capacity. At high current densities, surface-driven adsorption reactions became dominant, C@DSBC with a large surface area provides more electrochemical active sites to react with K^+. Similarly, Kang's group investigated the effect of particle size on the potassium storage mechanism of Bi metal.[43] As shown in Fig. 5a, nano-Bi with a size of ~15 nm shows an obvious solid-solution phase transition during the discharge process. In contrast, bulk-Bi with a size of ~250 nm exhibits equilibrium two-phase transformation with multiphase coexistence, which is similar to the previous report.[37] They proposed that the differences in phase transition mechanisms stem from variations in dynamics, the diffusion-controlled reaction fast ionic transport kinetics and homogeneous diffusion resulting in a highly reversible solid-solution phase transition (Fig. 5b). This work offers insight into the origin of the superior electrochemical performance of nanosized Bi electrodes.

The potassium storage performance of 2D-layered bismuthine was investigated by Wu and co-workers; they successfully

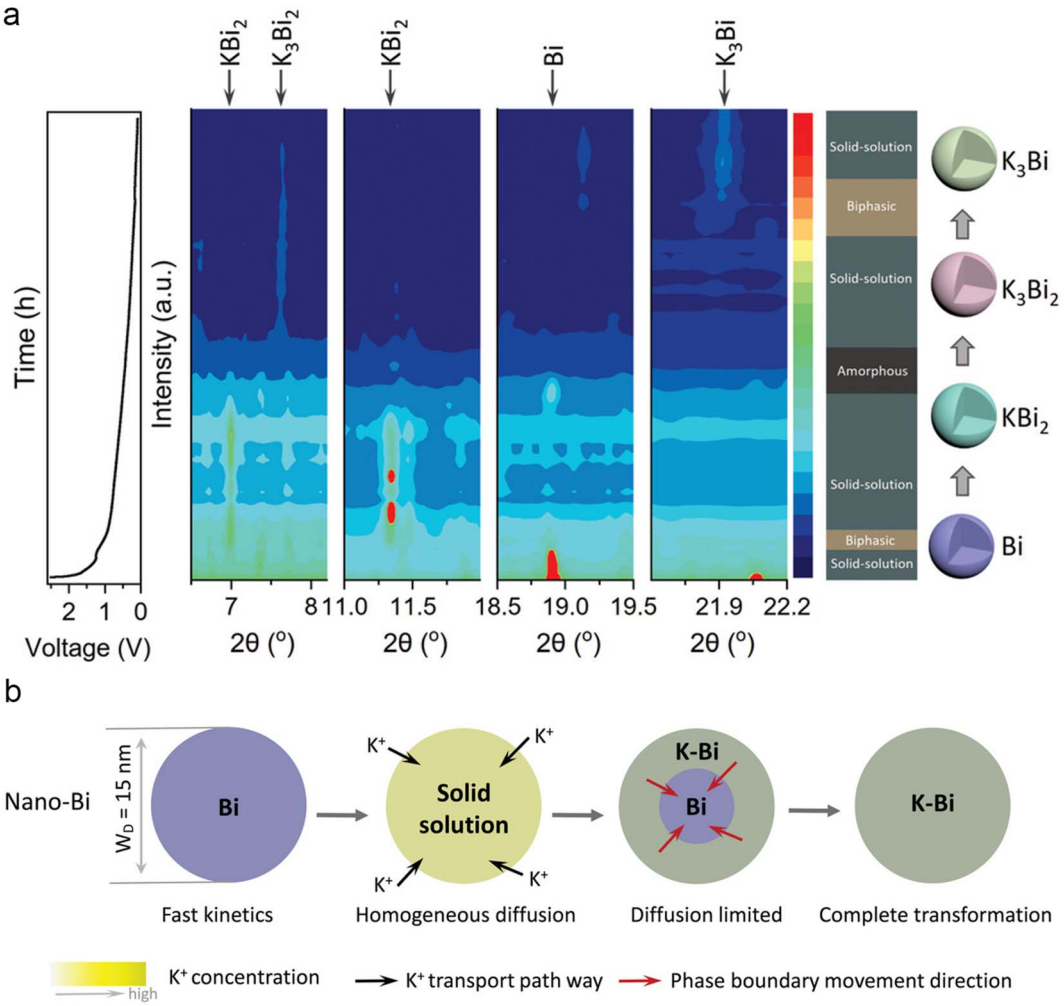

Fig. 5 (a) The voltage profile and corresponding contour plot of the *in situ* SXRD pattern of nano-Bi during the initial discharge process. (b) Schematic illustration of the potassiation mechanisms for nano-Bi. Reproduced with permission.[43] Copyright 2022, Wiley-VCH.

prepared ultra-thin few layered bismuthene nanosheets (FBNs) through the ultrasonication-assisted electrochemical exfoliation method.[44] The unique structure of FBNs not only facilitates the rapid diffusion of K^+ but also promotes the penetration of the electrolyte and mitigates the volume changes during the charge/discharge process. Benefiting from these advantages, FBNs deliver a high reversible capacity of 227 mA h g^{-1} at 15 A g^{-1}, and slight capacity decay after 2500 cycles. Noticeably, Yu's group systematically studied the impact of dimensionality on the potassium storage performance of bismuth anodes (Fig. 6a–d).[35] They successfully prepared a series of bismuth metal materials with different dimensions. All samples underwent noticeable morphological changes during the charge/discharge process, with the 0D, 1D, and 3D samples being encapsulated by the SEI layer and losing electrochemical activity (Fig. 6e, f and h). As shown in Fig. 6g, the two-dimensional bismuth metal (2D-Bi) transformed into continuous porous Bi nanoligaments and maintained a nanosheet morphology. This unique structure facilitates the shortening of the potassium ion transport path and alleviates volume changes. Therefore, the 2D-Bi exhibited the best rate performance and cycling stability (Fig. 6i). To demonstrate the practical application potential of the 2D-Bi, the PB cathode was applied to assemble full cells. The 2D-Bi//PB full cells deliver high energy density (174 W h kg^{-1}), along with excellent cycling stability (a capacity retention of 98.2% after 150 cycles). Although this work can provide some guidance for fundamental research, it is difficult to apply in practical application.

2.3 Hybridization with carbon materials

Hybridization with carbon materials not only leverages the high electrical conductivity and structural robustness of carbon materials but also capitalizes on their ability to facilitate rapid K^+ transport and accommodate huge volume changes during the charge/discharge process. In general, three dimensions of carbon materials (1D, 2D and 3D) are employed to improve the electrochemical performance of the bismuth anode. Lu's group applied Bi-based metal–organic frameworks (Bi-MOFs) as precursors to prepare ultrathin carbon film@carbon nanorods@Bi nanoparticle (UCF@CNs@BiN) composites.[45] The unique structure endows a fast ion transport channel and

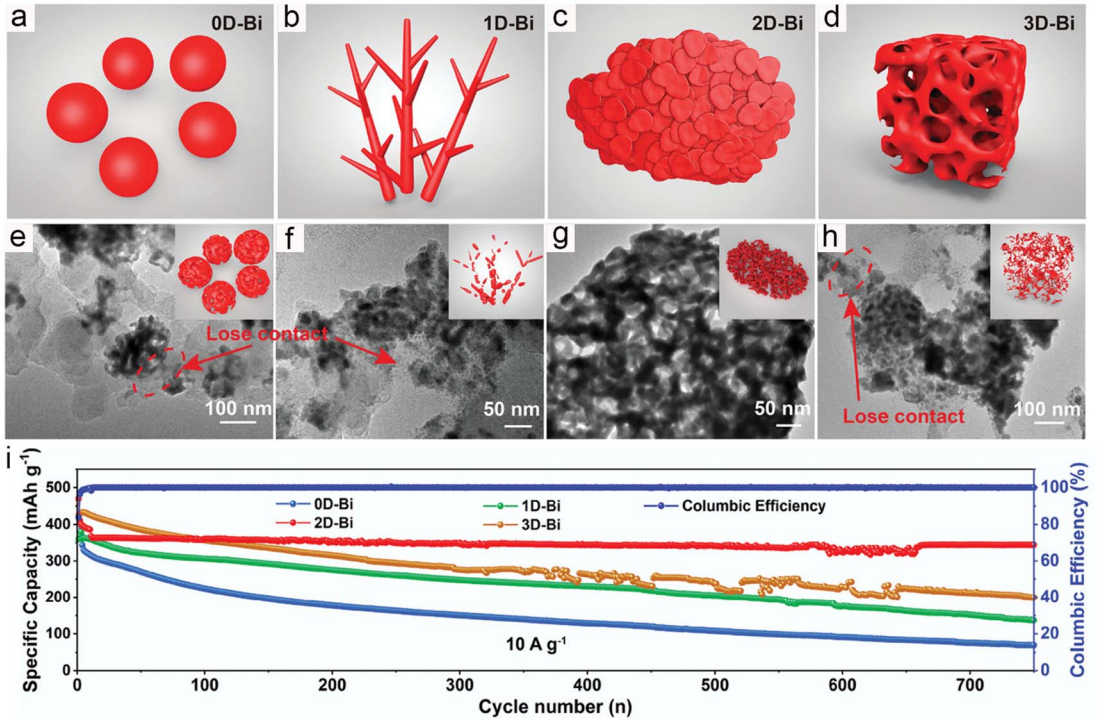

Fig. 6 (a–d) Schematic illustration and (e–h) post-cycle TEM images of the 0D-Bi, 1D-Bi, 2D-Bi, and 3D-Bi. Inset: schematic illustration of Bi in different dimensions after the charge/discharge process. (i) Cycling stability of Bi with different dimensionalities. Reproduced with permission.[35] Copyright 2021, Wiley-VCH.

buffers the volume change during the charge/discharge process. In addition, the UCF@CN matrix effectively avoids the side reaction between the Bi nanoparticles and electrolyte. Therefore, UCF@CNs@BiN composites show a superior potassium storage performance. Subsequently, Yin and co-workers prepared a self-standing electrode of ultrafine Bi nanoparticles encapsulated in porous carbon nanofibers (Bi/PCNFs) by simple electrospinning and following annealing.[46] The unique vessel-like mesopores of Bi/PCNFs are beneficial for mass (ion and electron) transport and electrolyte infiltration during the charge/discharge process. Meanwhile, the volume change of Bi nanoparticles was alleviated by PCNFs. Therefore, Bi/PCNFs show an excellent potassium storage performance. Recently, Zhao's group reported Bi/MWCNT (Bi nanoparticles

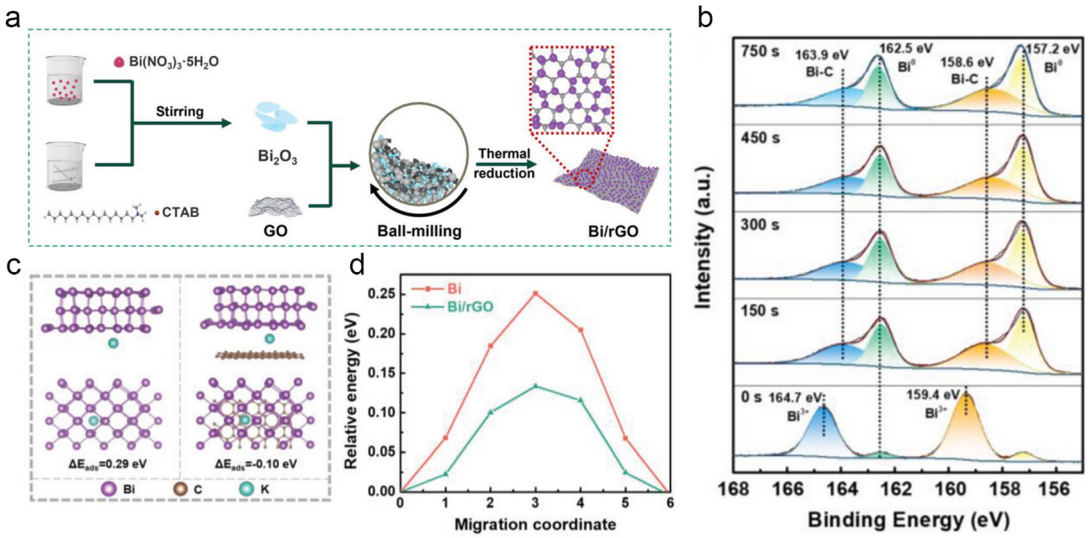

Fig. 7 (a) Schematic illustration for the preparation of Bi/rGO composites. (b) XPS Bi 4f spectra of Bi/rGO-2. (c) Potassium adsorption on the surface of Bi (012) and the interface of Bi/rGO. (d) The K^+ diffusion barrier energy in the Bi and Bi/rGO. Reproduced with permission.[51] Copyright 2024, Wiley-VCH.

were uniformly distributed in the 3D MWCNT networks) composites for PIBs.[47] The 3D MWCNT network effectively accelerated the electron and ion transport and mitigated volume changes.

Tai's group reported a hierarchical bismuth nanodots/graphene (BiND/G) nanoarchitecture for PIBs, the ultrafine nanodots with a size of ≈3 nm were uniformly dispersed on the graphene layers. The BiNDs provide more electrochemical reaction active sites and effectively reduce the ion transport length. The graphene layer avoids the agglomeration of BiNDs and accommodates the volume change during the charge/discharge process. Therefore, BiND/G electrodes show a satisfactory electrochemical performance. Subsequently, Guan and co-workers designed multicore–shell Bi@N-doped carbon (Bi@N–C) nanosheets, which own an interior void space to buffer the volume change.[48] They found that the Bi@N–C electrode exhibits a superior pseudocapacitance behavior and good structural stability. To obtain a high-volumetric capacity, Qiu's group prepared a flexible and free-standing Bi nanosheet/reduced graphene oxide (BiNS/rGO) composite membrane.[49] Noticeably, the porosity of BiNS/rGO is regulated by gas expansion and mechanical compression. BiNS/rGO-30 with porosity similar to the expansion ratio of BiNS after potassiation shows the best electrochemical performance, realizing a high reversible volumetric capacity of 451 mA h cm^{-3}. Recently, Xu *et al.* synthesized 2D bismuth@N-doped carbon sheets (2D Bi@NOC) with the Bi–O–C bond and internal void space by a self-template method.[50] *In situ* TEM reveals that the internal void space can buffer the volume change. In addition, the robust Bi–O–C bond plays a pivotal role in reducing the energy barrier for K^+ diffusion and facilitating thermodynamic K^+ adsorption. Benefiting from the above advantages, the 2D Bi@NOC electrode delivers a superior rate performance (220.6 mA h g^{-1} at 50 A g^{-1}) and excellent cycling stability (a high reversible capacity of 341.7 mA h g^{-1} was maintained even after 1000 cycles). Most recently, Xu's group proposed a unique Bi nanoparticles/reduced graphene oxide (Bi/rGO) composite for PIBs (Fig. 7a).[51] As shown in Fig. 7b, a unique strong interfacial Bi–C bonding between Bi and rGO was disclosed by XPS. The Bi–C bonds not only accelerate the interfacial charge transfer, but also avoid the aggregation of Bi nanoparticles and accommodate volume changes. Moreover, theoretical calculation demonstrated that the rGO plays a key role in improving the interfacial electron

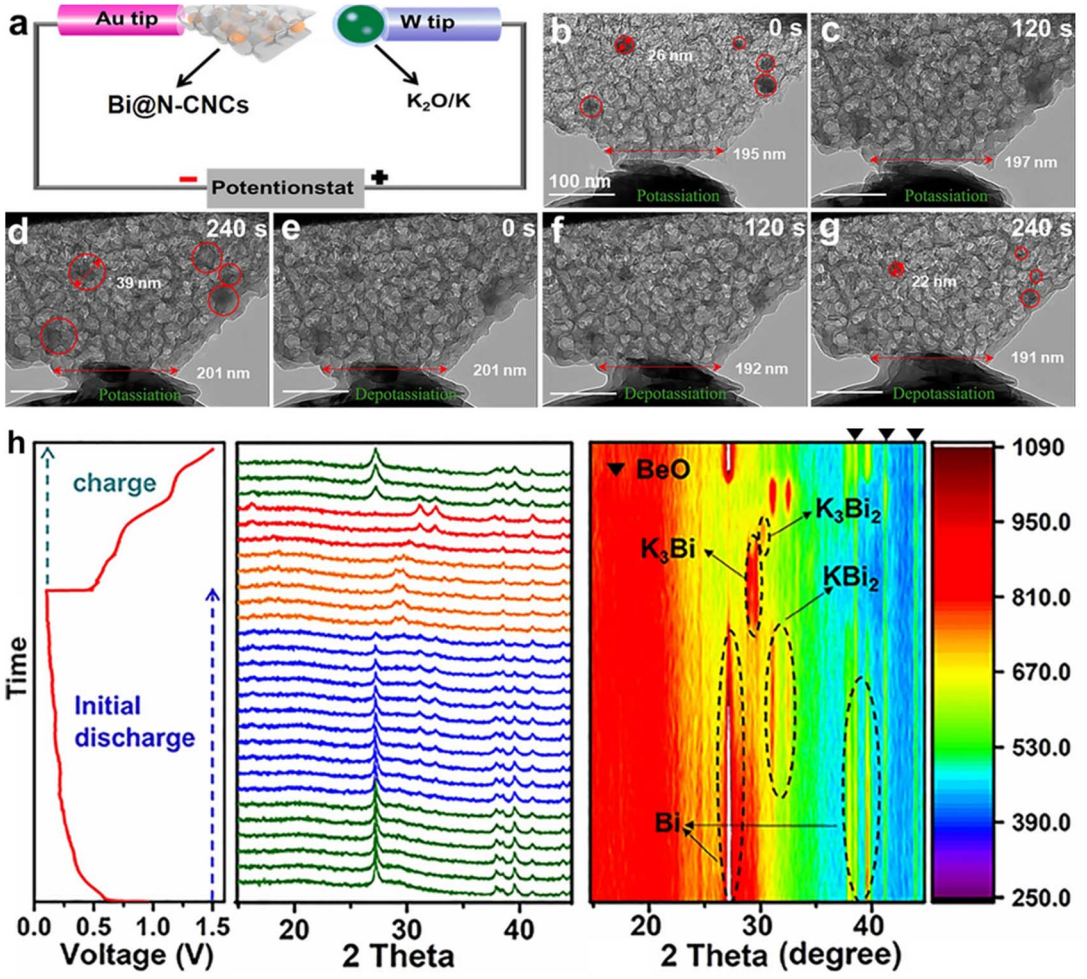

Fig. 8 (a) Schematic illustration of the *in situ* TEM nanobattery device. (b–g) Time-resolved TEM images of the 850-Bi@N–CNCs during the charge/discharge process. (h) *In situ* XRD of the 850-Bi@N–CNCs during the charge/discharge process. Reproduced with permission.[54] Copyright 2021, Wiley-VCH.

Table 1 The electrochemical performance of some representative Bi anode materials in PIBs

Materials	Initial discharge capacity (mA h g^{-1})/current density (A g^{-1})	Rate performance (mA h g^{-1})/current density (A g^{-1})	Cycling stability (capacity retention%/cycles)	Ref
Bi@3DGF	185.2/1	154.0/10	88.0/400	52
UCF@CNs@BiN	327.0/0.1	121.0/1	77.2/600	45
	121.0/1		74.8/700	
Bi@N–C	328.0/1	152.0/100	81.7/100	53
Bi@N–C	340.0/5	222.0/30	75.2/500	48
	320.0/10		56.3/1000	
BiNS/rGO-30	338/0.5	100.0/10	80.4/90	49
BiND/G	213.0/5	200/10	99.0/500	57
	200/10		88.0/500	
850-Bi@N–CNCs	224.0/5	235.5/10	95.3/1200	54
Bi@C	333.0/0.5	182.0/2	62/1000	58
Bi/PCNFs	220/1	163.3/5	77.7/1000	46
2D Bi@NOC	372.8/10	220.6/50	91.6/1000	50
Bi/PPy/CNT	361/0.1	267.7/3.2	83.6/200	55
Bi@N–C-800	267.0/1	255.0/2	100.0/400	59
Bi/MWCNTs-650	320.0/1	251.0/20	82.0/500	47
HD-Bi@G	364.7/1	271.0/40	75.0/2000	56
Bi@C-nanorods	205.0/1	138.0/2	-/500	60
C@DSBC	250.0/0.4	222.0/0.8	74/200	42
Bi∈NSC	313.0/5	298/6	91.0/1000	41
Bi@N-CT	304.0/3.85	297/7.7	88.0/1000	40
FBNs	351.4/7.5	182/20	90.5/100	44
2D-Bi	344.0/10	345/30	94.0/750	35
Bi@NS-C	402/1	399.5/20	88.0/800	61
Nano-Bi	141.0/0.5	52/2	52.4/550	43
Bi@rGO@NC	348.3/0.05	31.9/1	15.0/400	62

transfer and potassium adsorption capability, and decreases the K^+ diffusion energy barrier (Fig. 7c and d). Therefore, the Bi/rGO electrode delivers a high reversible capacity of 384.8 mA h g^{-1} and superior cycling stability (no obvious capacity decay after 1000 cycles).

For example, Yu's group synthesized a unique three-dimensional structure with Bi nanoparticles embedded in 3D macroporous graphene frameworks (Bi@3DGFs) through a space-confined super-assembly strategy.[52] The three-dimensional porous graphene framework facilitates the mitigation of volume changes during charge/discharge processes and enhances the wettability of the electrolyte, leading to improved electrode integrity and electrochemical reaction kinetics. Therefore, Bi@3DGFs deliver an unprecedented rate performance and cycling stability. Simultaneously, they reported a multicore-shell structured Bi@N-doped carbon (Bi@N–C) anode.[53] Subsequently, Bi NPs encapsulated in a 3D foam-like N-doped carbon nanocage (Bi@N–CNCs) framework with avoid space were synthesized by Yuan and co-workers.[54] They found that the calcination temperature was closely related to the potassium-storage performance of Bi@N–CNCs, and 850-Bi@N–CNCs with the large surface area ensure fast K^+ transfer to the abundant active sites. As shown in Fig. 8a–g, the N–CNCs can effectively accommodate the volume expansion of Bi NPs during the charge/discharge process. Moreover, a highly reversible alloying reaction of 850-Bi@N–CNCs was disclosed by *in situ* XRD (Fig. 8h). Therefore, 850-Bi@N–CNCs deliver a high capacity retention of 95.2% after 1200 cycles. More importantly, a high energy density of 170 W h kg^{-1} was achieved in 850-Bi@N–CNCs//$KFe[Fe(CN)_6$ full cells. Recently, a three-dimensional (3D) ternary bismuth nanoparticles/conductive polymers/carbon nanotubes (Bi/PPy/CNT) hybrid anode material was reported by Li's group.[55] The unique hydrogel network affords a fast electron transport path and enough porosity. Most recently, Li's group designed a 3D dense encapsulated architecture of 2D Bi nanosheets (HD-Bi@G) for PIBs.[56] The 3D high-conductivity elastic network can effectively accommodate the volume and avoid pulverization of electrodes during the charge/discharge process. Therefore, the HD-Bi@G electrode delivers a superior rate performance (271.0 mA h g^{-1} at 40 A g^{-1}) and cycling stability (a high capacity retention of 75% even after 2000 cycles). More importantly, the HD-Bi@G shows a high density of 2.3 g cm^{-3} enabling a high initial Coulombic efficiency (ICE) of 90.8% and volumetric capacity of 1032.2 mA h cm^{-3}. However, the density is relatively low for practical applications.

3. Conclusions and perspectives

Bi anode materials have been considered as potential candidates for high energy density PIBs due to their high theoretical capacity. In general, Bi anode materials suffer from huge volume changes during the charge/discharge process resulting in an inferior electrochemical performance. In this review, we systematically discuss the recent achievements and effective strategies to boost the potassium storage performance of Bi

anode materials. The electrochemical performance of some representative materials is summarized in Table 1. Hybridization with carbon materials effectively enhances the electronic conductivity of electrode materials and alleviates volume changes. However, the capacity contribution of carbon materials is negligible, and introducing too much carbon materials can lead to a decrease in the specific capacity of electrode materials. Morphology design can effectively shorten the K^+ transport path and maintain the integrity of the electrode, but it suffers from relatively complex fabrication processes and lower tap densities, which greatly limit its practical applications. In contrast, optimizing the electrolyte is a simpler process and can enable microsized bismuth anodes to achieve excellent electrochemical performance. Noticeably, the commonly used ether electrolytes typically show a low oxidation stability, which may pose challenges in compatibility with high-voltage cathodes when assembling potassium-ion full batteries. Recently, some novel ether-based electrolytes with high oxidation stability were applied in PIBs.[63,64] Therefore, developing novel high-voltage electrolytes with superior compatibility with bismuth anodes and high-voltage cathodes is of significant importance for the practical application of potassium-ion full batteries. In summary, these strategies are still in the laboratory stage, and their effectiveness in practical scenarios has yet to be further verified. We believe that combining thin carbon coating technology with advanced electrolytes can enable the practical application of bismuth anodes in PIBs. However, it is still necessary to compare the electrochemical performance with the graphite anodes (in pouch and cylindrical batteries with high-loading electrodes) to evaluate their potential for practical application.

To realize the practical application of bismuth anodes in potassium-ion batteries, we believe future research should focus on the following aspects: First, morphological design and hybridization with carbon materials can effectively enhance electrochemical performance. However, complex fabrication processes hinder their practical application. Developing methods for large-scale preparation is of significant importance for promoting the practical application of these two strategies. Second, the electrode/electrolyte interface significantly impacts the electrochemical performance of the electrolyte materials. Designing novel electrolytes to improve the electrochemical performance of bismuth anodes represents a crucial approach. Last, the performance evaluation of bismuth anodes should not be limited to small-capacity coin cells but should include the assembly of large-capacity pouch and cylindrical cells to assess their potential for practical applications.

Data availability

The data supporting the findings of this study are available within the article.

Author contributions

X. Z. and X. C. performed the literature search, analyzed the published results, and wrote the manuscript. W. K., X. Z., X. W. and X. C. structured this review. C. Z., L. L. and S. C. provided key advice and supervised the preparation of the text.

Conflicts of interest

There are no conflicts to declare.

Acknowledgements

This work was supported by the National Natural Science Foundation of China (52202286, 22309002, 52250710680, 52171217, and 52172173), Natural Science Foundation of Zhejiang Province (LY24B030006), High-end Foreign Experts Recruitment Plan of China (G2023016009L), Key Research and Development Program of Zhejiang Province (2023C011232), Science and Technology Project of State Grid Corporation of China (5419-202158503A-0-5-ZN), Basic Research Project of Wenzhou City (G20220016), Science and Technology Plan Project of Wenzhou Municipality (ZG2022032), Anhui Provincial Natural Science Foundation (2308085QB55), Excellent Research and Innovation Team Project of Anhui Province (2022AH010001), and China Postdoctoral Science Foundation (2023M730007).

References

1 M. Li, J. Lu, Z. Chen and K. Amine, *Adv. Mater.*, 2018, **30**, 1800561.
2 Z. Fan, X. Zhou, J. Qiu, Z. Yang, C. Lei, Z. Hao, J. Li, L. Li, R. Zeng and S.-L. Chou, *Angew. Chem., Int. Ed.*, 2023, **62**, e202308888.
3 C. D. Quilty, D. Wu, W. Li, D. C. Bock, L. Wang, L. M. Housel, A. Abraham, K. J. Takeuchi, A. C. Marschilok and E. S. Takeuchi, *Chem. Rev.*, 2023, **123**, 1327–1363.
4 X. Zhou, Y. Huang, B. Wen, Z. Yang, Z. Hao, L. Li, S.-L. Chou and F. Li, *Proc. Natl. Acad. Sci. U. S. A.*, 2024, **121**, e2316914121.
5 S. Liu, L. Kang and S. C. Jun, *Adv. Mater.*, 2021, **33**, 2004689.
6 Z. Zhang, M. Song, C. Si, W. Cui and Y. Wang, *eScience*, 2023, **3**, 100070.
7 Y. Wu, Z. Zhao, X. Hao, R. Xu, L. Li, D. Lv, X. Huang, Q. Zhao, Y. Xu and Y. Wu, *Carbon Neutralization*, 2023, **2**, 551–573.
8 X. Zhou, B. Wen, Y. Cai, X. Chen, L. Li, Q. Zhao, S.-L. Chou and F. Li, *Angew. Chem., Int. Ed.*, 2024, **63**, e202402342.
9 M. Jiang, C. Fu, P. Meng, J. Ren, J. Wang, J. Bu, A. Dong, J. Zhang, W. Xiao and B. Sun, *Adv. Mater.*, 2022, **34**, e2102026.
10 Z. Hao, X. Shi, W. Zhu, X. Zhang, Z. Yang, L. Li, Z. Hu, Q. Zhao and S. Chou, *Chem. Sci.*, 2022, **13**, 11376–11381.
11 J. Y. Hwang, S. T. Myung and Y. K. Sun, *Adv. Funct. Mater.*, 2018, **28**, 1704294.
12 M. Okoshi, Y. Yamada, S. Komaba, A. Yamada and H. Nakai, *J. Electrochem. Soc.*, 2016, **164**, A54–A60.
13 L. Li, S. Zhao, Z. Hu, S.-L. Chou and J. Chen, *Chem. Sci.*, 2021, **12**, 2345–2356.
14 A. Eftekhari, *J. Power Sources*, 2004, **126**, 221–228.

15 L. Duan, C. Shao, J. Liao, L. Song, Y. Zhang, R. Li, S. Guo, X. Zhou and H. Zhou, *Angew. Chem., Int. Ed.*, 2024, **63**, e202400868.
16 L. Li, Z. Hu, Q. Liu, J.-Z. Wang, Z. Guo and H.-K. Liu, *Cell Rep. Phys. Sci.*, 2021, **2**, 100531.
17 L. Zhou, Z. Cao, W. Wahyudi, J. Zhang, J.-Y. Hwang, Y. Cheng, L. Wang, L. Cavallo, T. Anthopoulos, Y.-K. Sun, H. N. Alshareef and J. Ming, *ACS Energy Lett.*, 2020, **5**, 766–776.
18 L. Li, Z. Hu, Y. Lu, C. Wang, Q. Zhang, S. Zhao, J. Peng, K. Zhang, S.-L. Chou and J. Chen, *Angew. Chem., Int. Ed.*, 2021, **60**, 13050–13056.
19 B. Ji, W. Yao, Y. Zheng, P. Kidkhunthod, X. Zhou, S. Tunmee, S. Sattayaporn, H. M. Cheng, H. He and Y. Tang, *Nat. Commun.*, 2020, **11**, 1225.
20 L. Fan, R. Ma, J. Wang, H. Yang and B. Lu, *Adv. Mater.*, 2018, **30**, e1805486.
21 Z. Xiao, F. Xia, L. Xu, X. Wang, J. Meng, H. Wang, X. Zhang, L. Geng, J. Wu and L. Mai, *Adv. Funct. Mater.*, 2021, **32**, 2108244.
22 Z. Jian, W. Luo and X. Ji, *J. Am. Chem. Soc.*, 2015, **137**, 11566–11569.
23 Y. Lu, Q. Zhang, L. Li, Z. Niu and J. Chen, *Chem*, 2018, **4**, 2786–2813.
24 C. Li, A. Bi, H. Chen, Y. Pei, M. Zhao, C. Yang and Q. Jiang, *J. Mater. Chem. A*, 2021, **9**, 5740–5750.
25 M. Sha, L. Liu, H. Zhao and Y. Lei, *Carbon Energy*, 2020, **2**, 350–369.
26 J. Jia, X. Lu, C. Yang and Q. Jiang, *J. Mater. Chem. A*, 2024, **12**, 1359.
27 X. Du and B. Zhang, *ACS Nano*, 2021, **15**, 16851–16860.
28 X. Du, Y. Gao and B. Zhang, *Adv. Funct. Mater.*, 2021, **31**, 2102562.
29 X. Liu, Y. J. Sun, Y. Tong and H. Y. Li, *Small*, 2022, **18**, 2204045.
30 X. Xiang, D. Liu, X. Zhu, K. Fang, K. Zhou, H. Tang, Z. Xie, J. Li, H. Zheng and D. Qu, *Appl. Surf. Sci.*, 2020, **514**, 145947.
31 X. Liu, X. Yu, Y. Tong, Y. Sun, W. Mai, L. Niu and H. Li, *Chem. Eng. J.*, 2022, **446**, 137329.
32 Q. Zhang, J. Mao, W.-K. Pang, T. Zheng, V. Sencadas, Y. Chen, Y. Liu and Z. Guo, *Adv. Energy Mater.*, 2018, **8**, 1703288.
33 R. Zhang, J. Bao, Y. Wang and C.-F. Sun, *Chem. Sci.*, 2018, **9**, 6193–6198.
34 K. Lei, C. Wang, L. Liu, Y. Luo, C. Mu, F. Li and J. Chen, *Angew. Chem., Int. Ed.*, 2018, **57**, 4687–4691.
35 X. Cheng, Y. Sun, D. Li, H. Yang, F. Chen, F. Y. Huang, Y. Jiang, Y. Wu, X. An and Y. Yu, *Adv. Energy Mater.*, 2021, **11**, 2102263.
36 S. Chu, K. Lei, Q. Yang, J. Li, Y. Zhao, M. Gu, L. Li, X. Hu, Y. Zhang, Z. Chen, S. Shi, S.- L Chou and S. Zheng, *Sci. China Chem.*, 2024, DOI: **10.1007/s11426-024-2071-y**.
37 J. Huang, X. Lin, H. Tan and B. Zhang, *Adv. Energy Mater.*, 2018, **8**, 1703496.
38 X. Xiang, D. Liu, X. Zhu, Y. Wang, D. Qu, Z. Xie, X. Zhang and H. Zheng, *ACS Appl. Mater. Interfaces*, 2022, **14**, 34722–34732.
39 Q. Zhang, H. Wei, L. Wang, J. Wang, L. Fan, H. Ding, J. Lei, X. Yu and B. Lu, *ACS App. Mater. Interfaces*, 2019, **11**, 44352–44359.
40 H. Li, C. Zhao, Y. Yin, Y. Zou, Y. Xia, Q. An, Z. Jian and W. Chen, *Nanoscale*, 2020, **12**, 4309–4313.
41 T. Jiao, S. Wu, J. Cheng, D. Chen, D. Shen, H. Wang, Z. Tong, H. Li, B. Liu, J.-J. Kai, C.-S. Lee and W. Zhang, *J. Mater. Chem. A*, 2020, **8**, 8440–8446.
42 F. Xie, L. Zhang, B. Chen, D. Chao, Q. Gu, B. Johannessen, M. Jaroniec and S.-Z. Qiao, *Matter*, 2019, **1**, 1681–1693.
43 J. Zhang, G. Kim, M. Park, J. L. Zhang, S. Lee, Y. X. Cui, K. Zhang, F. Zou and Y. M. Kang, *Adv. Energy Mater.*, 2022, **12**, 2202446.
44 C. Shen, T. Cheng, C. Liu, L. Huang, M. Cao, G. Song, D. Wang, B. Lu, J. Wang, C. Qin, X. Huang, P. Peng, X. Li and Y. Wu, *J. Mater. Chem. A*, 2020, **8**, 453–460.
45 S. Su, Q. Liu, J. Wang, L. Fan, R. Ma, S. Chen, X. Han and B. Lu, *ACS Appl. Mater. Interfaces*, 2019, **11**, 22474–22480.
46 D. D. Ouyang, C.-Y. Wang, H. Zhu, F. Yu and J. Yin, *ACS Appl. Nano Mater.*, 2022, **5**, 13171–13179.
47 J. Yu, D. Zhao, C. S. Ma, L. Feng, Y. Zhang, L. Zhang, Y. Liu and S. Guo, *J. Colloid Interface Sci.*, 2023, **643**, 409–419.
48 X. Shi, J. Zhang, Q. Yao, R. Wang, H. Wu, Y. Zhao and L. Guan, *J. Mater. Chem. A*, 2020, **8**, 8002–8009.
49 L. Zeng, M. Liu, P. Li, G. Zhou, P. Zhang and L. Qiu, *Sci. China Mater.*, 2020, **63**, 1920–1928.
50 A. Xu, Q. Zhu, G. Li, C. Gong, X. Li, H. Chen, J. Cui, S. Wu, Z. Xu and Y. Yan, *Small*, 2022, **18**, 2203976.
51 Y. Wei, P. Zhang, S. J. Zhou, X. Tian, R. A. Soomro, H. Liu, H. Du and B. Xu, *Small*, 2024, 2306541.
52 X. Cheng, D. Li, Y. Wu, R. Xu and Y. Yu, *J. Mater. Chem. A*, 2019, **7**, 4913–4921.
53 H. Yang, R. Xu, Y. Yao, S. Ye, X. Zhou and Y. Yu, *Adv. Funct. Mater.*, 2019, **29**, 1809195.
54 Z. Sun, Y. Liu, W. Ye, J. Zhang and C. Yuan, *Angew. Chem., Int. Ed.*, 2021, **133**, 7256–7263.
55 W. Zhang, X. Chen, H. Xu, Y. Liu, X. Zhao, Z. Zhang and L. Li, *Chin. J. Chem.*, 2022, **40**, 1585–1591.
56 B. Wang, L. Shi, Y. Zhou, X. Wang, X. Liu, D. Shen, Q. Yang, S. Xiao, J. Zhang and Y. Li, *Small*, 2024, e2310736.
57 Y. Zhao, X. Ren, Z. Xing, D. Zhu, W. Tian, C. Guan, Y. Yang, W. Qin, J. Wang, L. Zhang, Y. Huang, W. Wen, X. Li and R. Tai, *Small*, 2020, **16**, 1905789.
58 J. Yao, C. Zhang, G. Yang, M. Sha, Y. Dong, Q. Fu, Y. Wu, H. Zhao, M. Wu and Y. Lei, *ACS Appl. Mater. Interfaces*, 2021, **13**, 31766–31774.
59 R. Ababaikeri, Y. Sun, X. C. Wang, X. F. Li, M. H. Li, F. Zhang, Y. Li, P. Y. Wang, J. X. cGuo and Y. L. Cao, *J. Alloys Compd.*, 2023, **935**, 168207.
60 S. Qi, X. Xie, X. Peng, D. H. L. Ng, M. Wu, Q. Liu, J. Yang and J. Ma, *Phys. Status Solidi RRL*, 2019, **13**, 1900209.
61 H. Long, X. Yin, X. Wang, Y. Zhao and L. Yan, *J. Energy Chem.*, 2022, **67**, 787–796.
62 S. Qiao, Y. Liu, K. Wang and S. Chong, *Batteries*, 2023, **9**, 505.
63 M. Gu, X. Zhou, Q. Yang, S. Chu, L. Li, J. Li, Y. Zhao, X. Hu, S. Shi, Z. Chen, Y. Zhang, S. -L Chou and K. Lei, *Angew. Chem., Int. Ed.*, 2024, e202402946.
64 Z. Yu, K. Fan, Q. Liu, D. Wang, C. Chen, Y. Zhu, H. Huang and B. Zhang, *Adv. Funct. Mater.*, 2024, **34**, 2315446.